Supplementary Materials:

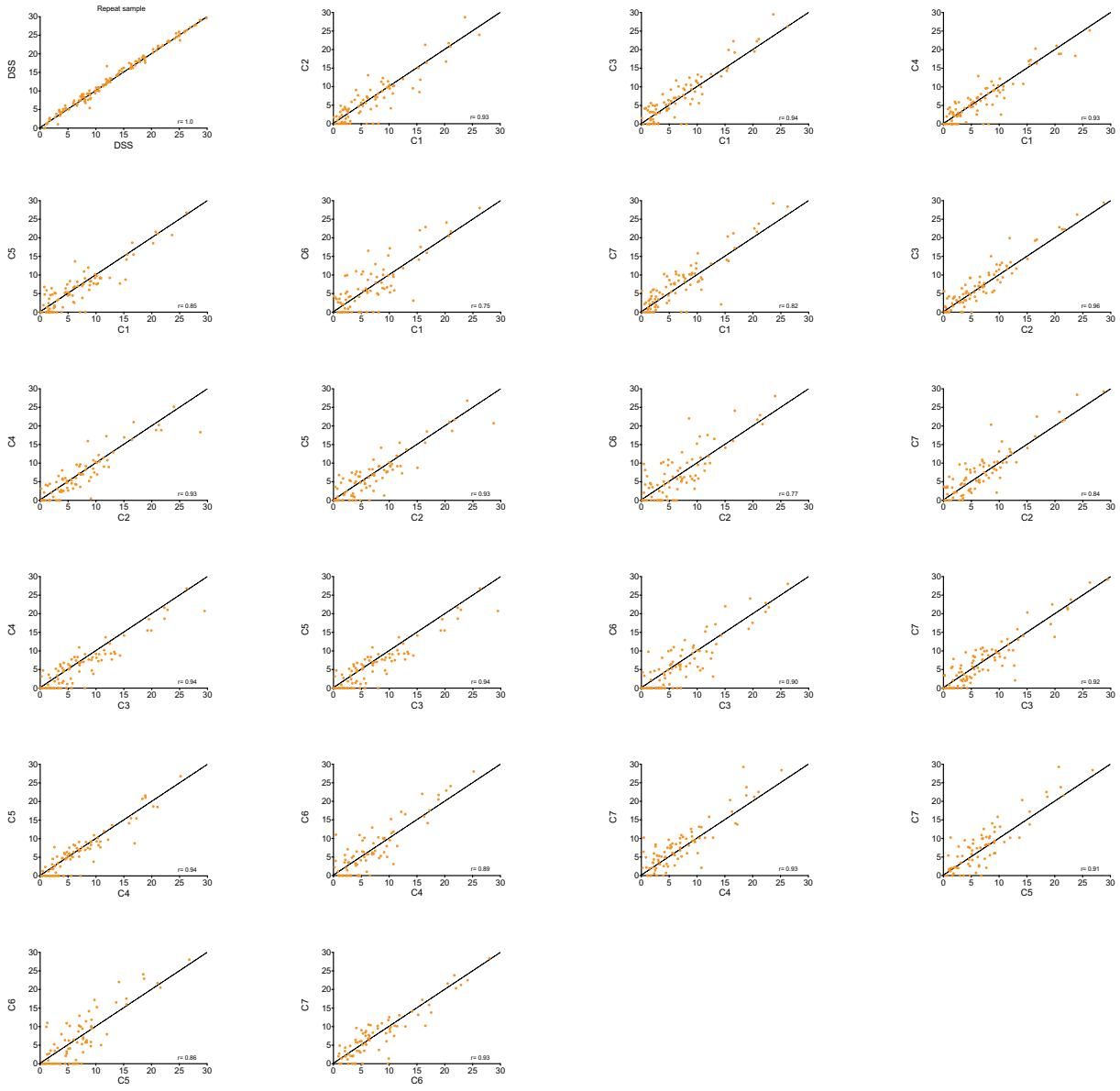

Supplementary Fig. S1. DSRT results from sample replicates as well as from different healthy donor controls show excellent correlation. DSS scatterplot of a patient sample screened twice and DSS scatterplot of each of the 7 healthy donor samples against each other. The dashed line corresponds to equal scores in the compared screens to illustrate differential DSS values.

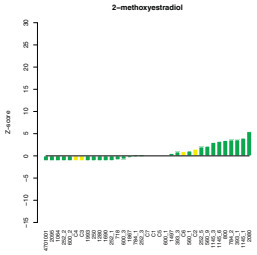
2−methoxyestradiol
Z-score

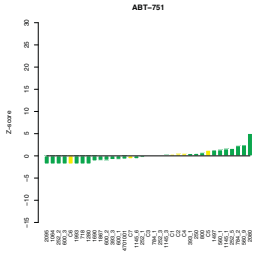
ABT−751
Z-score

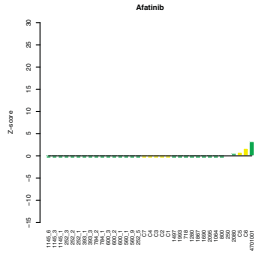
Afatinib
Z-score

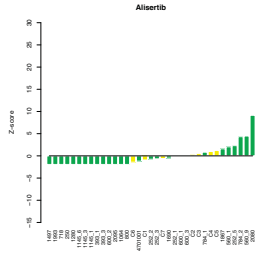
Alisertib
Z-score

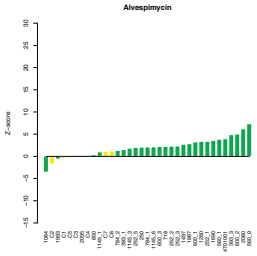
Alvespimycin
Z-score

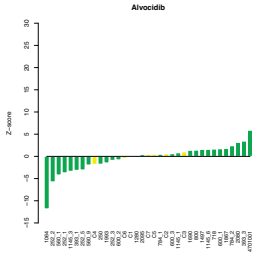
Alvocidib
Z-score

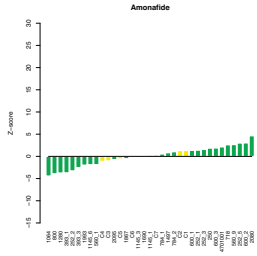
Amonafide
Z-score

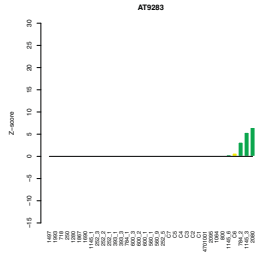
AT9283
Z-score

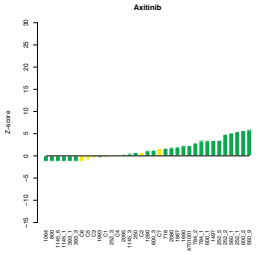
Axitinib
Z-score

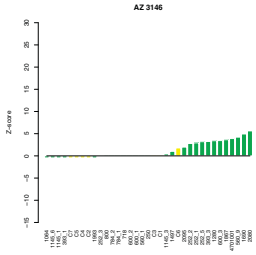
AZ 3146
Z-score

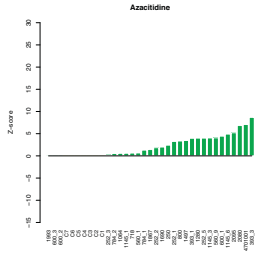
Azacitidine
Z-score

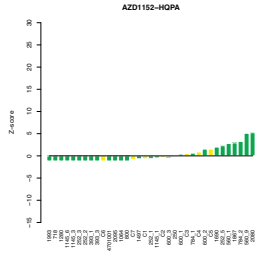
AZD1152−HQPA
Z-score

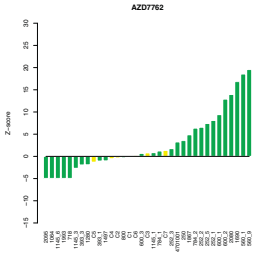
AZD7762
Z-score

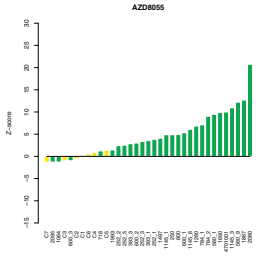
AZD8055
Z-score

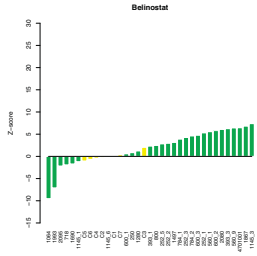
Belinostat
Z-score

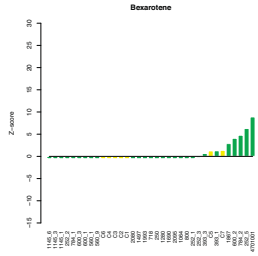
Bexarotene
Z-score

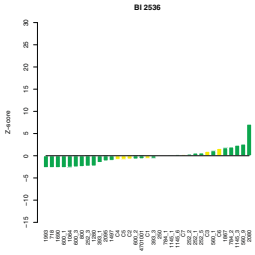
BI 2536
Z-score

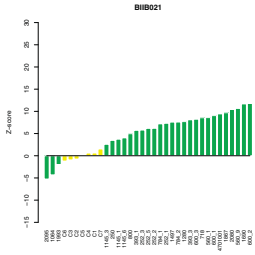
BIIB021
Z-score

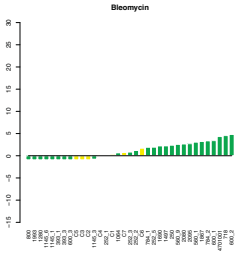
Bleomycin
Z-score

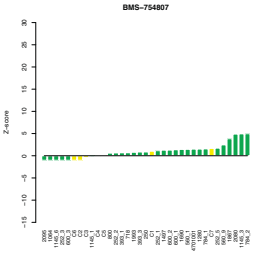
BMS−754807
Z-score

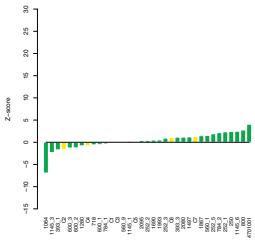
Bortezomib
Z-score

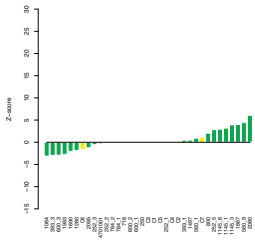
Camptotechin
Z-score

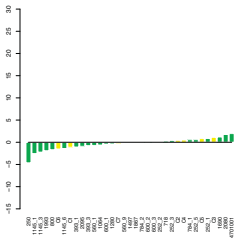
Canertinib
Z-score

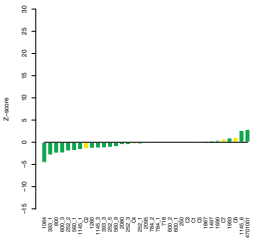
Carfilzomib
Z-score

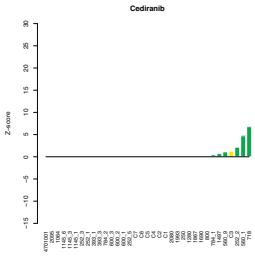
Cediranib
Z-score

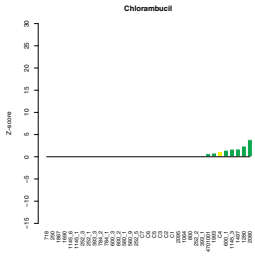
Chlorambucil
Z-score

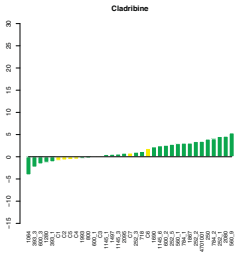
Cladribine
Z-score

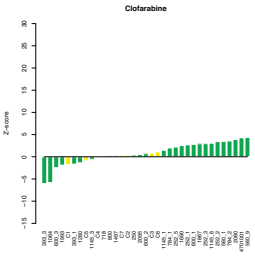
Clofarabine
Z-score

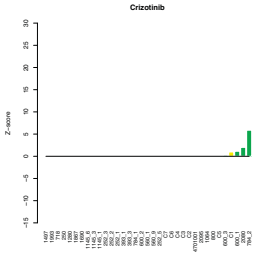
Crizotinib
Z-score

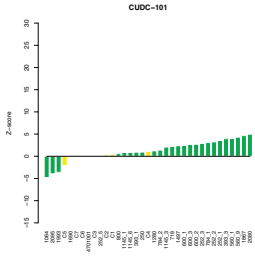
CUDC−101
Z-score

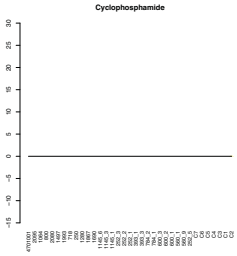
Cyclophosphamide
Z-score

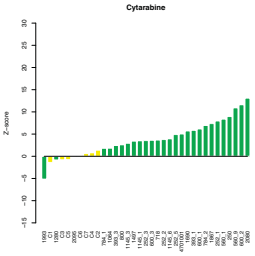
Cytarabine
Z-score

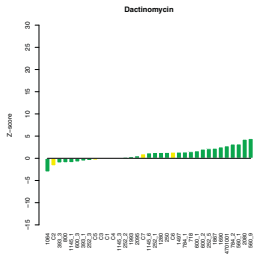
Dactinomycin
Z-score

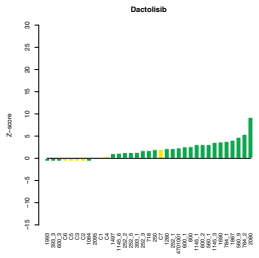
Dactolisib
Z-score

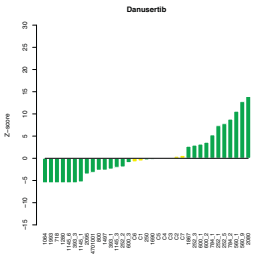
Danusertib
Z-score

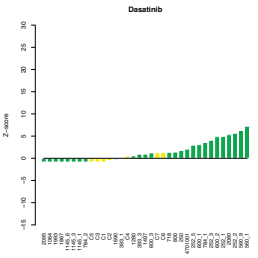
Dasatinib
Z-score

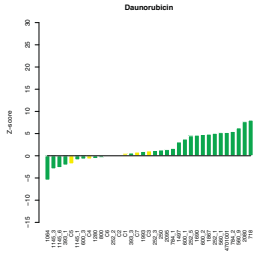
Daunorubicin
Z-score

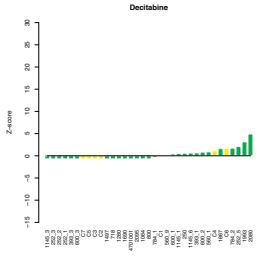
Decitabine
Z-score

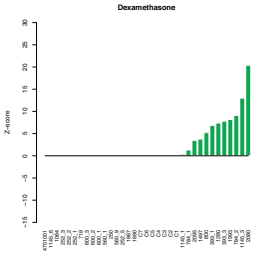
Dexamethasone
Z-score

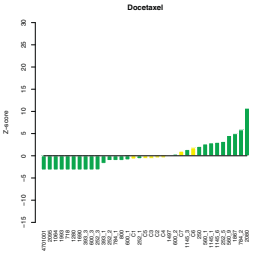
Docetaxel
Z-score

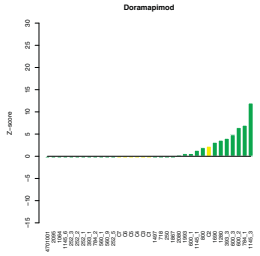
Doramapimod
Z-score

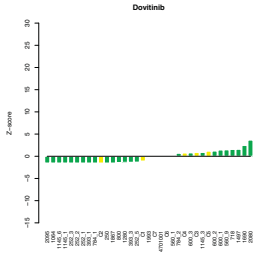
Dovitinib
Z-score

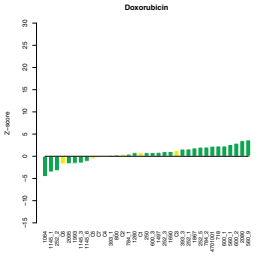
Doxorubicin
Z-score

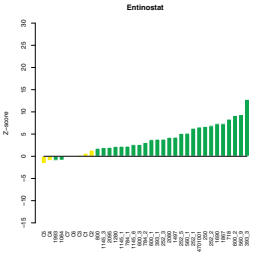
Entinostat
Z-score

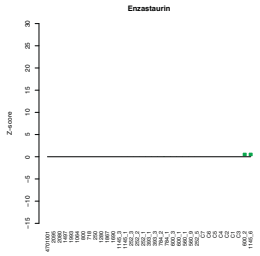
Enzastaurin
Z-score

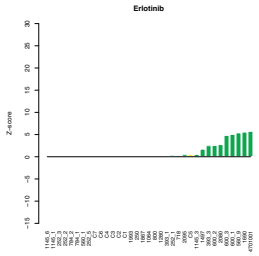
Erlotinib
Z-score

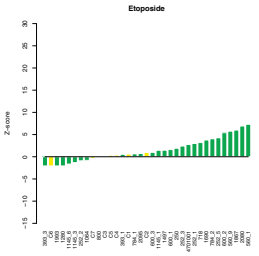
Etoposide
Z-score

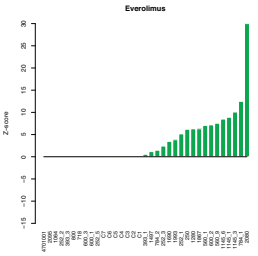
Everolimus
Z-score

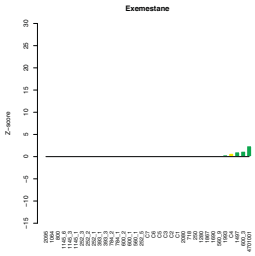
Exemestane
Z-score

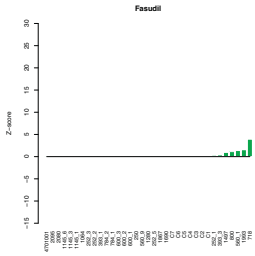
Fasudil
Z-score

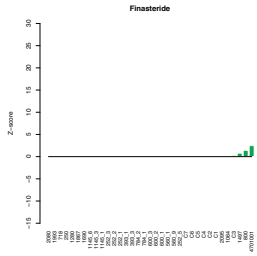
Finasteride
Z-score

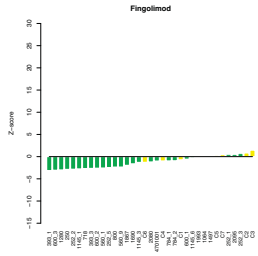
Fingolimod
Z-score

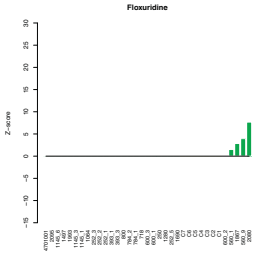
Floxuridine
Z-score

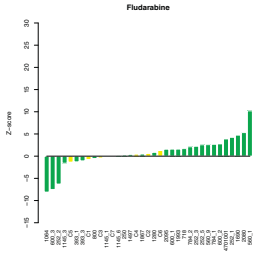
Fludarabine
Z-score

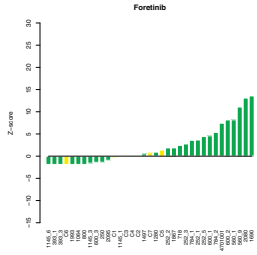
Foretinib
Z-score

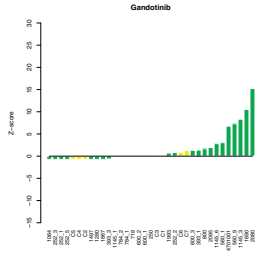
Gandotinib
Z-score

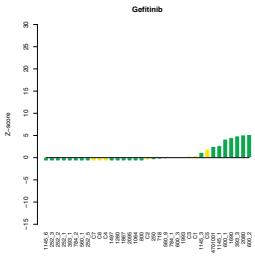
Gefitinib
Z-score

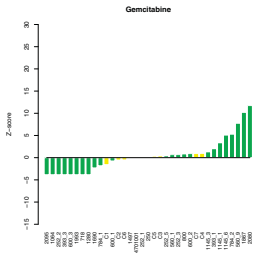
Gemcitabine
Z-score

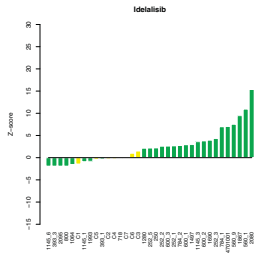
Idelalisib
Z-score

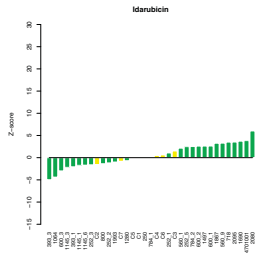
Idarubicin
Z-score

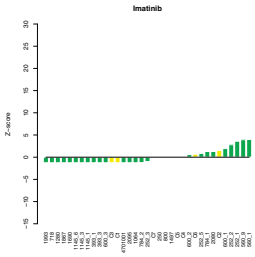
Imatinib
Z-score

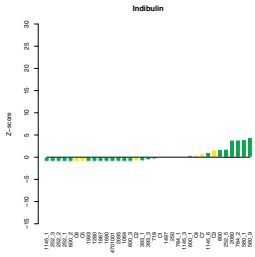
Indibulin
Z-score

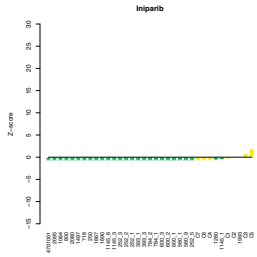
Iniparib
Z-score

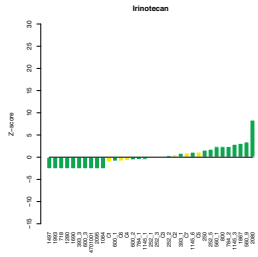
Irinotecan
Z-score

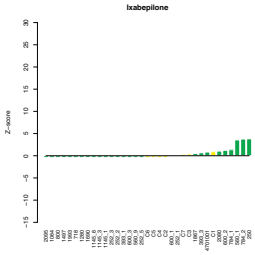
Ixabepilone
Z-score

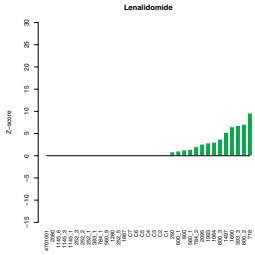
Lenalidomide
Z-score

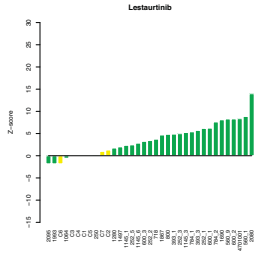
Lestaurtinib
Z-score

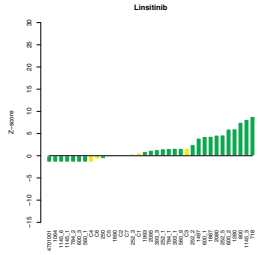
Linsitinib
Z-score

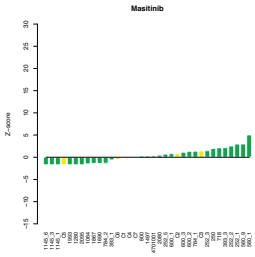
Masitinib
Z-score

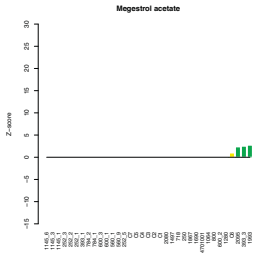
Megestrol acetate
Z-score

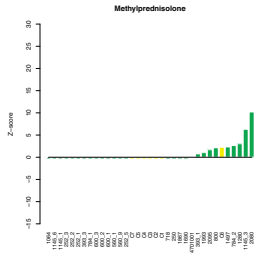
Methylprednisolone
Z-score

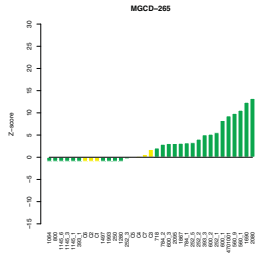
MGCD−265
Z-score

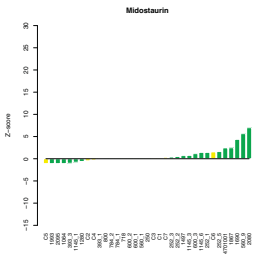
Midostaurin
Z-score

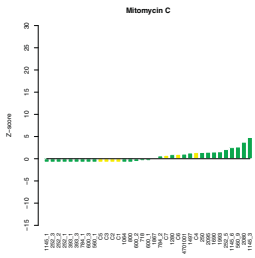
Mitomycin C
Z-score

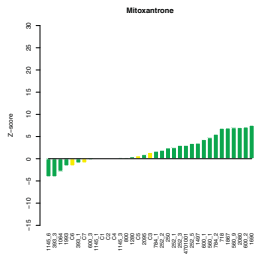
Mitoxantrone
Z-score

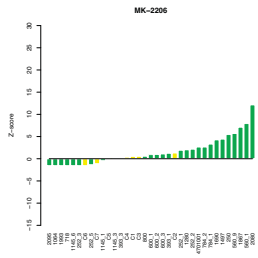
MK−2206
Z-score

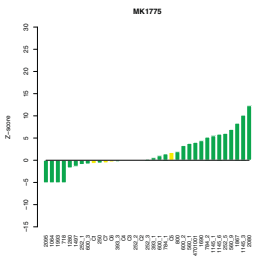
MK1775
Z-score

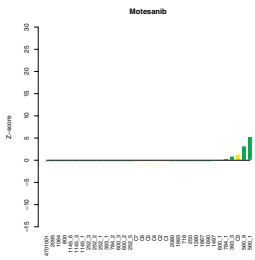
Motesanib
Z-score

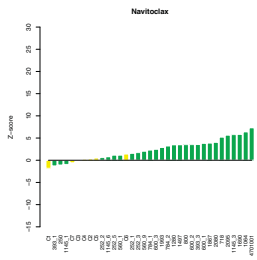
Navitoclax
Z-score

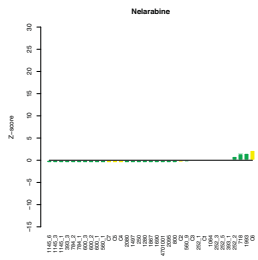
Nelarabine
Z-score

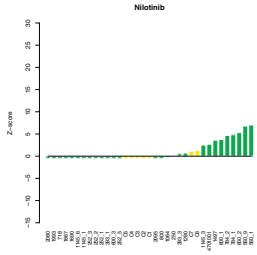
Nilotinib
Z−score

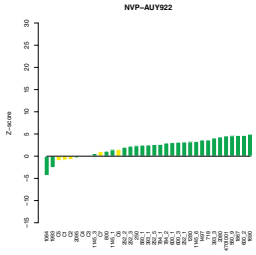
NVP−AUY922
Z−score

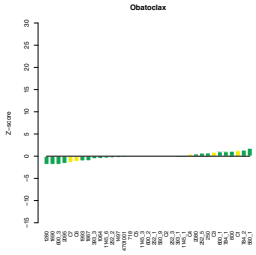
Obatoclax
Z−score

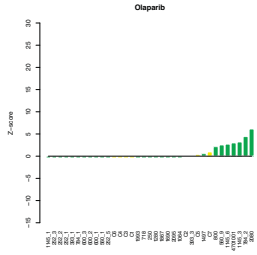
Olaparib
Z−score

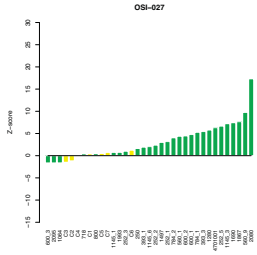
OSI−027
Z−score

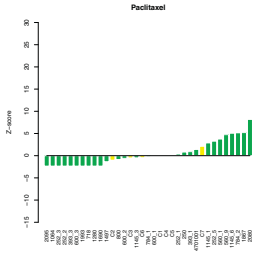
Paclitaxel
Z−score

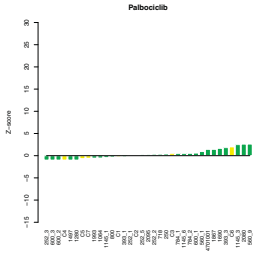
Palbociclib
Z−score

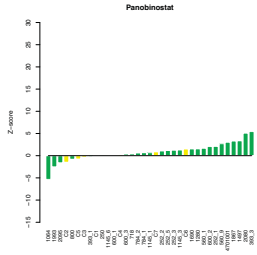
Panobinostat
Z−score

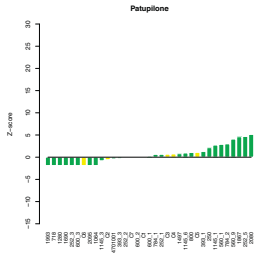
Patupilone
Z−score

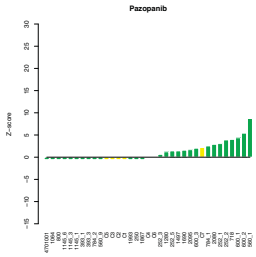
Pazopanib
Z−score

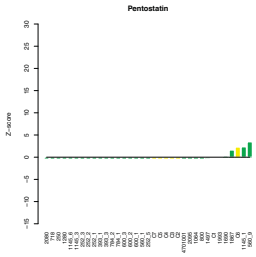
Pentostatin
Z−score

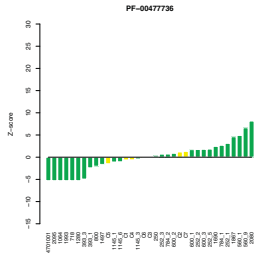
PF−00477736
Z−score

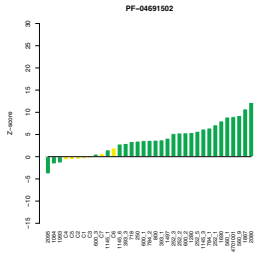
PF−04691502
Z−score

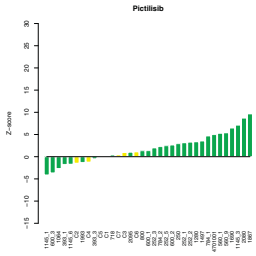
Pictilisib
Z−score

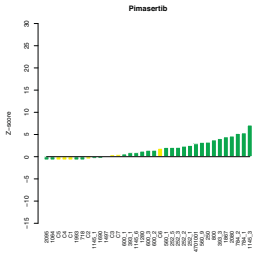
Pimasertib
Z−score

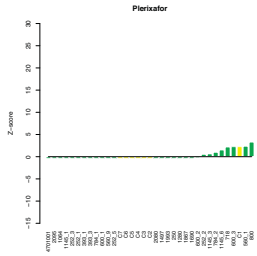
Plerixafor
Z−score

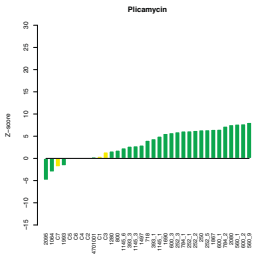
Plicamycin
Z-score

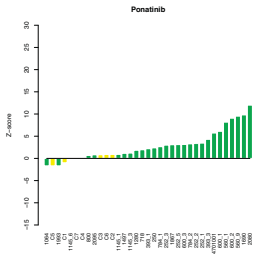
Ponatinib
Z-score

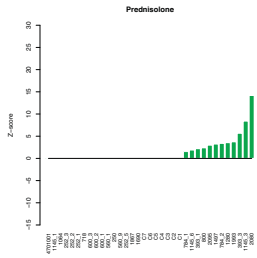
Prednisolone
Z-score

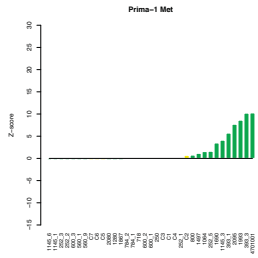
Prima−1 Met
Z-score

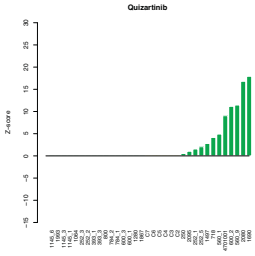
Quizartinib
Z-score

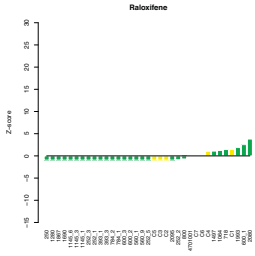
Raloxifene
Z-score

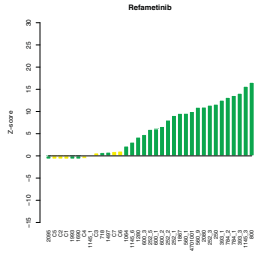
Refametinib
Z-score

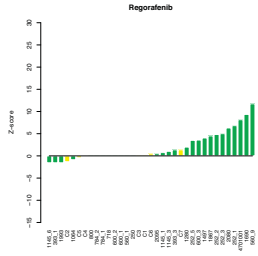
Regorafenib
Z-score

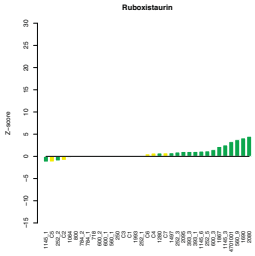
Ruboxistaurin
Z-score

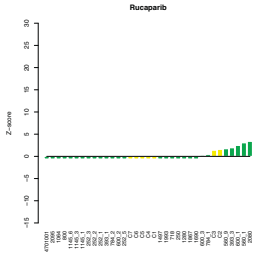
Rucaparib
Z-score

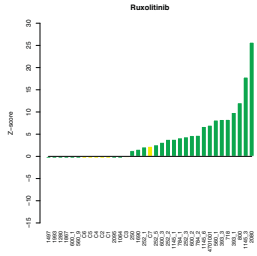
Ruxolitinib
Z-score

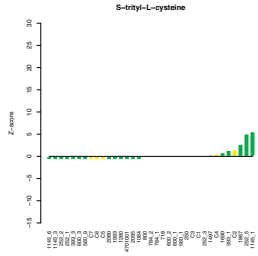
S−trityl−L−cysteine
Z-score

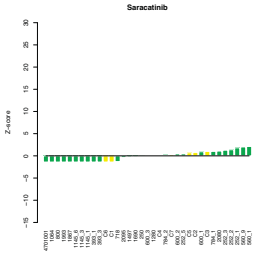
Saracatinib
Z-score

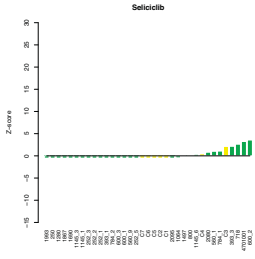
Seliciclib
Z-score

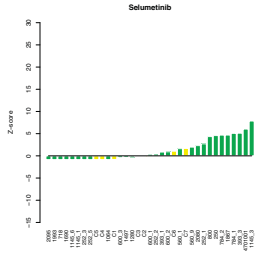
Selumetinib
Z-score

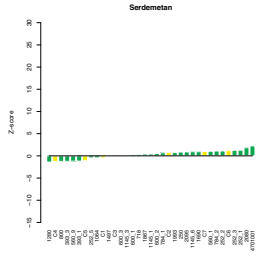
Serdemetan
Z-score

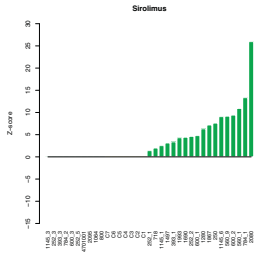
Sirolimus
Z-score

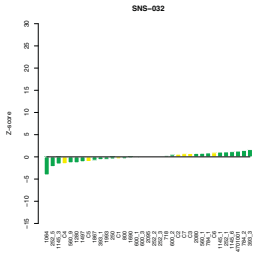
SNS−032
Z-score

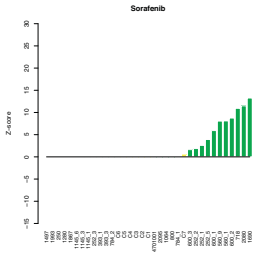
Sorafenib
Z-score

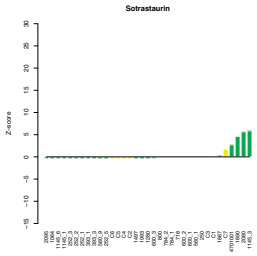
Sotrastaurin
Z-score

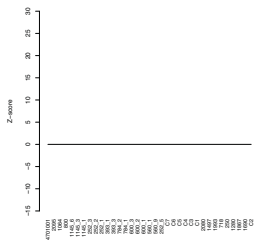
Streptozocin
Z-score

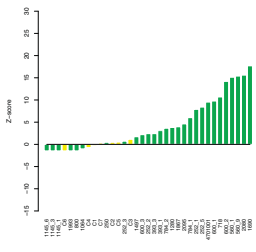
Sunitinib
Z-score

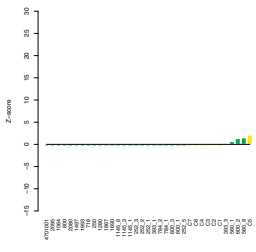
Tacedinaline
Z-score

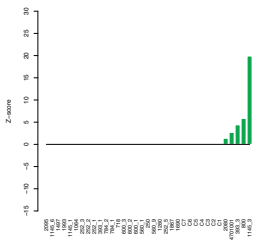
Tacrolimus
Z-score

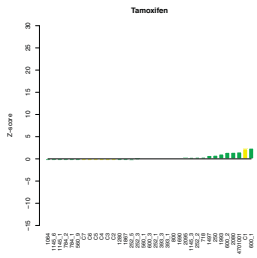
Tamoxifen
Z-score

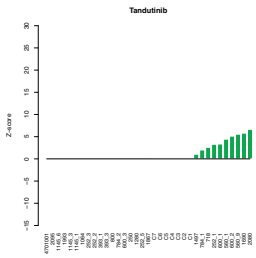
Tandutinib
Z-score

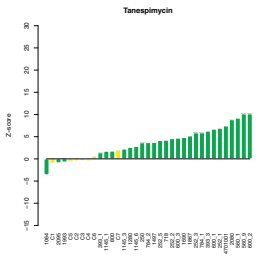
Tanespimycin
Z-score

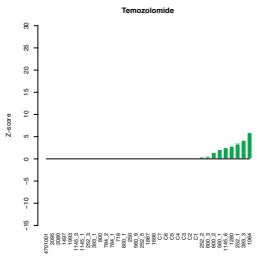
Temozolomide
Z-score

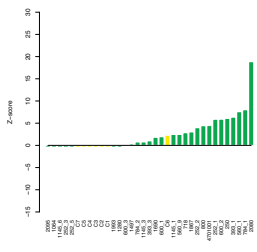
Temsirolimus
Z-score

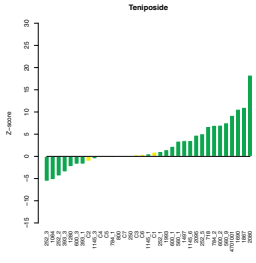
Teniposide
Z-score

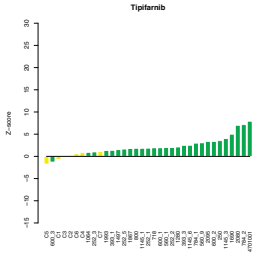
Tipifarnib
Z-score

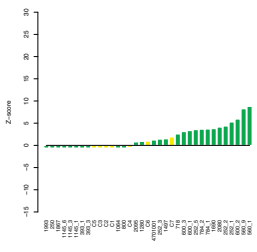
Tivozanib
Z-score

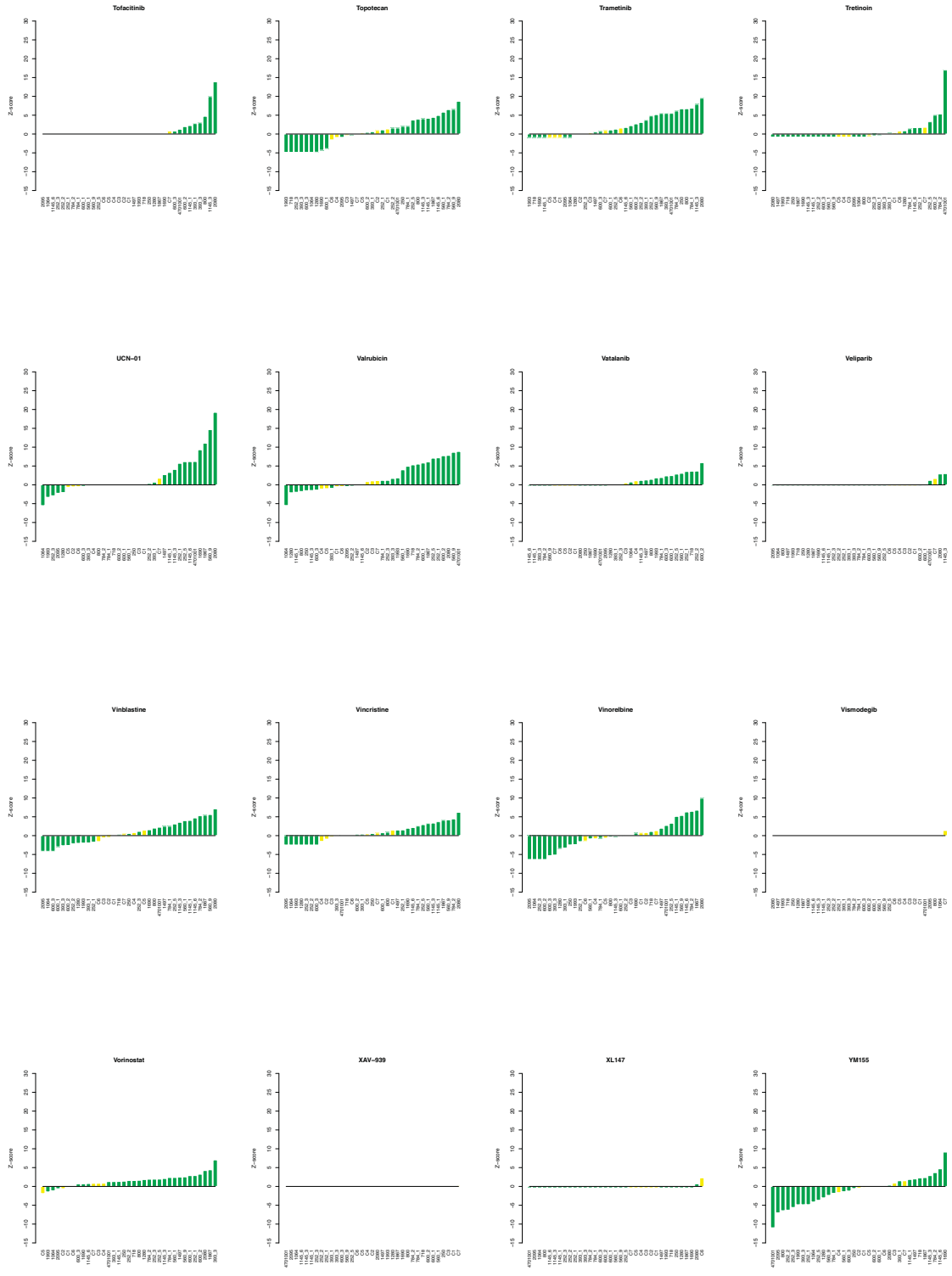

Supplementary Fig. S2. Distribution of drug sensitivity in AML and control samples. DSRT data represented as Z-scores (standard deviations from average control DSS drug response) identifies subgroups of AML patient samples exhibiting selective responses to anti-cancer agents.

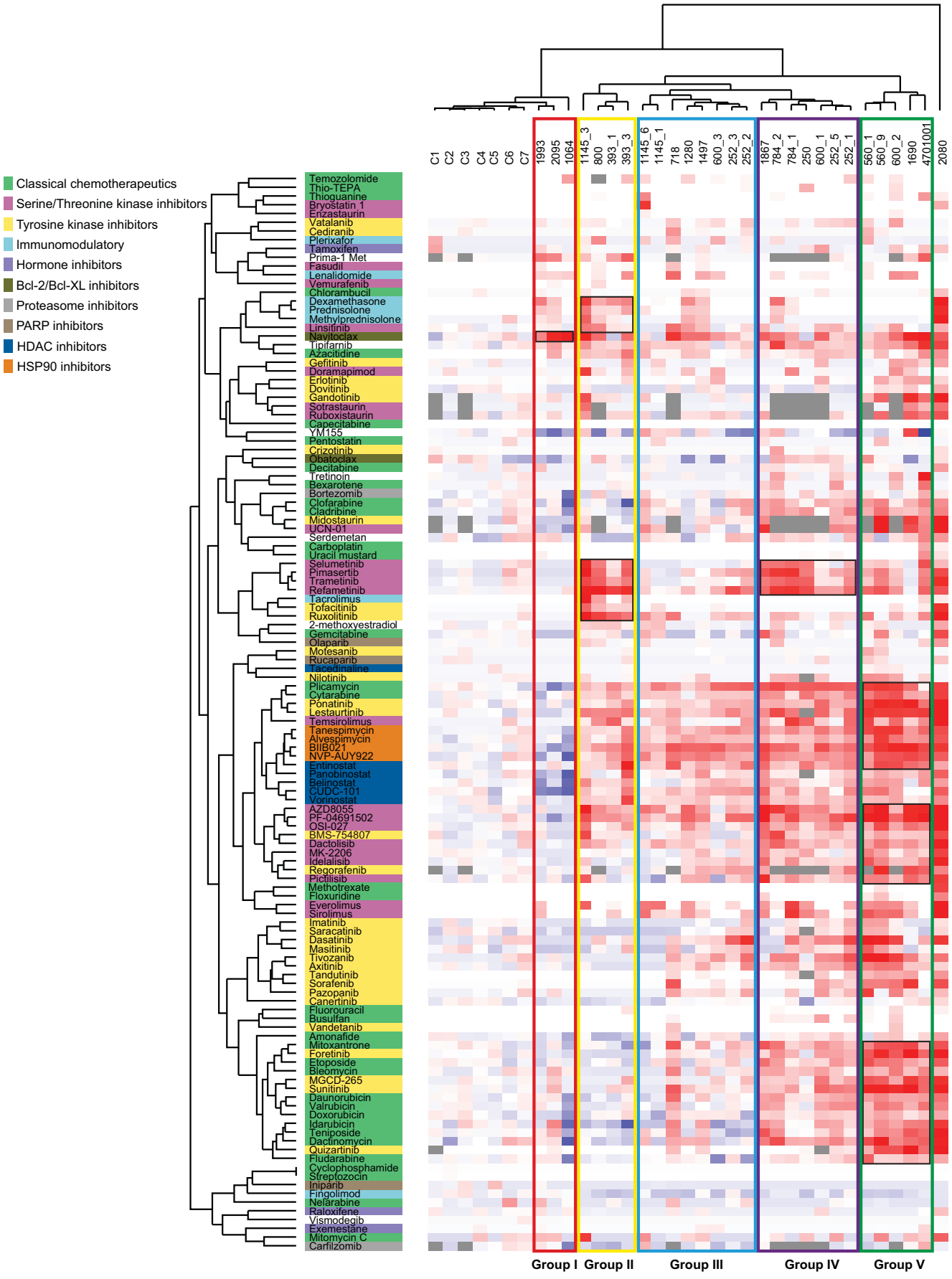
Classical chemotherapeutics
Serine/Threonine kinase inhibitors
Tyrosine kinase inhibitors
Immunomodulatory
Hormone inhibitors
Bcl-2/Bcl-XL inhibitors
Proteasome inhibitors
PARP inhibitors
HDAC inhibitors
HSP90 inhibitors
Temozolomide
Thio-TEPA
Thioguanine
Bryostatin 1
Enzastaurin
Vatalanib
Cediranib
Plerixafor
Tamoxifen
Prima-1 Met
Fasudil
Lenalidomide
Vemurafenib
Chlorambucil
Dexamethasone
Prednisolone
Methylprednisolone
Linsitinib
Navitoclax
Tipifarnib
Azacitidine
Gefitinib
Doramapimod
Erlotinib
Dovitinib
Gandotinib
Sotrastaurin
Ruboxistaurin
Capecitabine
YM155
Pentostatin
Crizotinib
Obatoclax
Decitabine
Tretinoin
Bexarotene
Bortezomib
Clofarabine
Cladribine
Midostaurin
UCN-01
Serdemetan
Carboplatin
Uracil mustard
Selumetinib
Pimasertib
Trametinib
Refametinib
Tacrolimus
Tofacitinib
Ruxolitinib
2-methoxyestradiol
Gemcitabine
Olaparib
Motesanib
Rucaparib
Tacedinaline
Nilotinib
Plicamycin
Cytarabine
Ponatinib
Lestaurtinib
Temsirolimus
Tanespimycin
Alvespimycin
BIIB021
NVP-AUY922
Entinostat
Panobinostat
Belinostat
CUDC-101
Vorinostat
AZD8055
PF-04691502
OSI-027
BMS-754807
Dactolisib
MK-2206
Idelalisib
Regorafenib
Pictilisib
Methotrexate
Floxuridine
Everolimus
Sirolimus
Imatinib
Saracatinib
Dasatinib
Masitinib
Tivozanib
Axitinib
Tandutinib
Sorafenib
Pazopanib
Canertinib
Fluorouracil
Busulfan
Vandetanib
Amonafide
Mitoxantrone
Foretinib
Etoposide
Bleomycin
MGCD-265
Sunitinib
Daunorubicin
Valrubicin
Doxorubicin
Idarubicin
Teniposide
Dactinomycin
Quizartinib
Fludarabine
Cyclophosphamide
Streptozocin
Iniparib
Fingolimod
Nelarabine
Raloxifene
Vismodegib
Exemestane
Mitomycin C
Carfilzomib
C1
C2
C3
C4
C5
C6
C7
1993
2095
1064
1145_3
800
393_1
393_3
1145_6
1145_1
718
1280
1497
600_3
252_3
252_2
1867
784_2
784_1
250
600_1
252_5
252_1
560_1
560_9
600_2
1690
4701001
2080
Group I
Group II
Group III
Group IV
Group V

Supplementary Fig. S3. *Ex vivo* anti-cancer sensitivity testing classifies AML patient samples in five functional groups. Unsupervised hierarchical clustering of DSRT results reflecting sensitivity to 123 of the 187 drugs (vertical axis) is visualized as a heatmap across 28 individual samples from AML patients and seven healthy bone marrow controls (horizontal axis). Sensitive drugs are shown in red based on a selective drug sensitivity score (sDSS) with blue indicating drugs that have more activity in the controls as opposed to the patient samples. Spearman and Euclidian distance measures were applied to DSS values of compounds and samples, respectively, that were clustered with complete linkage clustering method. This method provides a data-driven way to classify samples based on DSS (red, yellow, blue, purple and green boxes, corresponding to the five taxonomic classes described in Figure 3) and compounds based on their differential bioactivity across patient samples. The analysis reveals that several classes of drugs show selectivity in a subset of patient samples (black boxes). The compounds have also been colored to reflect their primary mode of action. Antimitotic compounds that were invariably active against most of the AML samples as well as compounds that were inactive in all the samples were excluded from this cluster analysis.

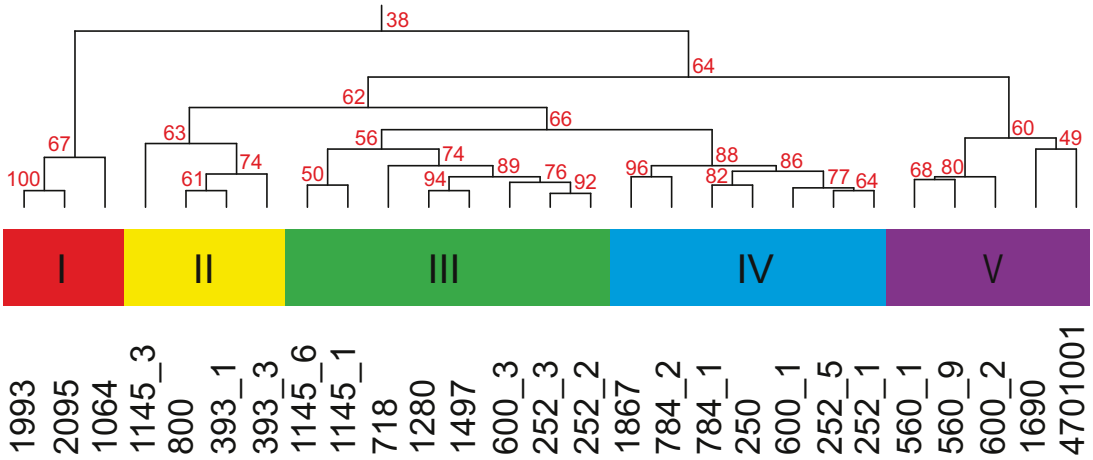

Supplementary Fig. S4. Reproducibility of the drug response subtypes detected using unsupervised hierarchical clustering of the DSRT results presented in Figure 3 and Supplementary Figure S3. The reproducibility of the DSRT clusters was assessed by randomly resampling 10,000 bootstrap samples of the original DSRT data and calculating the frequency that each cluster appears in the hierarchical clustering of the bootstrap replicates. The numbers in the dendrogram tree indicate the approximately unbiased (AU) empirical frequencies (0-100%) from the multi-scale bootstrap resampling implemented in the Pvclust R-package. Certain patient samples form outlier subgroups, thereby reducing the overall reproducibility of the DSRT clustering, but the majority of the drug response subclusters show high reproducibility values, indicating robustness of the response subtypes.

A

Patient 600

FLT3-ITD #1 (42 bp) 600_0

CAATTTAGGTATGAAAGCCAGCTACAGATGGTACAGGTGACCGGCTCCTCAGATAATGAGT
ACTTCTACGTGAGTCAGCCGACCGGCTCCTCAGATAATGAGTACTTCTACGTTGATTTCAGA
GAATATGAATATGATCTCAAATGGGAGTTTCCAAGAGAAAATTTAGAGTTTG

FLT3-ITD #2 (57 bp) 600_2

CAATTTAGGTATGAAAGCCAGCTACAGATGGTACAGGTGACCGGCTCCTCAGATAATGAGT
ACTTCTACGTTGATTTCAGAGAATATGAATATGATCTCAAATGGGAGTTTCCAAGAGAAAAT
TTAGAGTTCGATGGAGAATATGAATATGATCTCAAATGGGAGTTTCCAAGAGAAAATTTAGA
GTTTG

B

600 sample	Day	FLT3-ITD #1 (42 bp)	FLT3-ITD #2 (57 bp)
600_0	0	100.000%*	3.200%
	49	0.800%	3.800%
	56	0.080%	NA
	90	0.050%	NA
600_2	150	0.001-0.05%	100.000%*
600_3	221	NA	NA

Supplementary Fig. S5. Sequences of the FLT3-ITDs in exon 14 of patient 600. (**A**) Normal sequence of exon 14 is shown in turquoise, duplicated regions are shown in yellow, the normal instance of the duplicated sequence is underlined and the junction reads are highlighted in red. (**B**) qPCR MRD assay results for FLT3-ITD for patient 600 are depicted as the relative amount of each FLT3-ITD reported as a percentage of the amount detected in a reference sample (indicated by *). N/A indicates no sample material left for retrospective qPCR analysis.

A

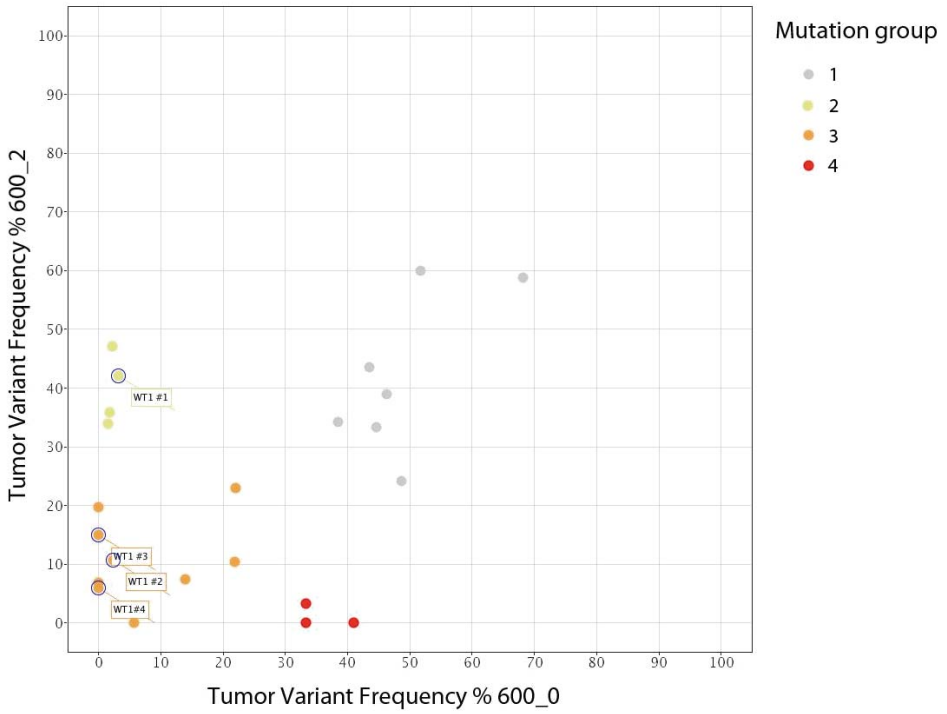

B

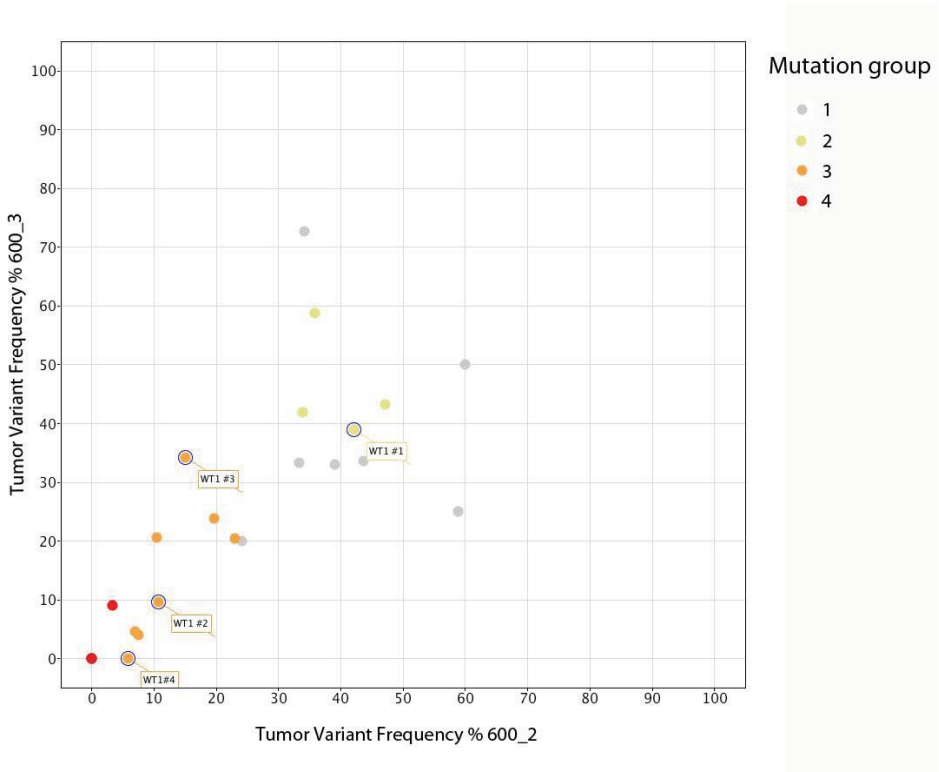

Supplementary Fig. S6. Tumor variant frequency in patient 600. (**A**) Tumor variant frequency percentages of sample 600_0 plotted against frequencies in sample 600_2. (**B**) Tumor variant frequencies in 600_2 plotted against frequencies in sample 600_3.

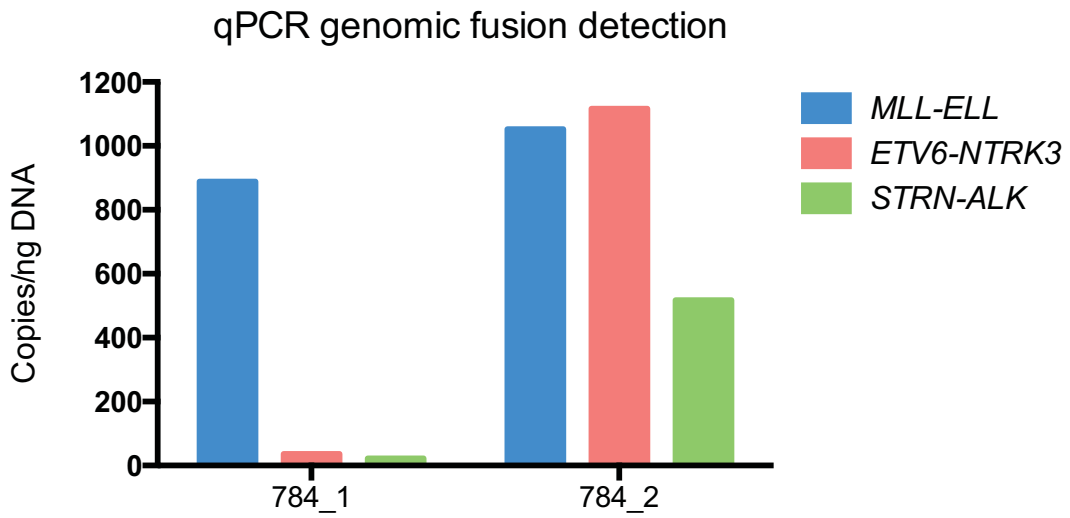

Supplementary Fig. S7. Copies/ng DNA of the genomic fusions detected by qPCR analysis in-patient 784.

ETV6-NTRK3

Sanger sequencing result of junction (reverse and complementary):

TGGTGCAGTGGGCTGGCTGAGTCCTCCTCACCACTGATGACAGCCACGGG
ACCTGCTATTCTCCCAATGGGCATGGCGTGCTCTTCAGGCGGGGAGA

Alignment of predicted fusion protein sequence:

```
fusion       1  MSETPAQCSIKQERISYTPPESPVPSYASSTPLHVPVPRALRMEEDSIRLPAHLRLQPIY   60
TEL          1  MSETPAQCSIKQERISYTPPESPVPSYASSTPLHVPVPRALRMEEDSIRLPAHLRLQPIY   60
TrkC             ------------------------------------------------------------

fusion      61  WSRDDVAQWLKWAENEFSLRPIDSNTFEMNGKALLLLTKEDFRYRSPHSGDVLYELLQHI  120
TEL         61  WSRDDVAQWLKWAENEFSLRPIDSNTFEMNGKALLLLTKEDFRYRSPHSGDVLYELLQHI  120
TrkC             ------------------------------------------------------------

fusion     121  LKQRKPRILFSPFFHPGNSIHTQPEVILHQNHEEDNCVQRTPRPSVDNVHHNPPTIELLH  180
TEL        121  LKQRKPRILFSPFFHPGNSIHTQPEVILHQNHEEDNCVQRTPRPSVDNVHHNPPTIELLH  180
TrkC             ------------------------------------------------------------

fusion     181  RSRSPITTNHRPSPDPEQRPLRSPLDNMIRRLSPAERAQGPRPHQENNHQESYPLSVSPM  240
TEL        181  RSRSPITTNHRPSPDPEQRPLRSPLDNMIRRLSPAERAQGPRPHQENNHQESYPLSVSPM  240
TrkC             ------------------------------------------------------------

fusion     241  ENNHCPASSESHPKPSSPRQESTRVIQLMPSPIMHPLILNPRHSVDFKQSRLSEDGLHRE  300
TEL        241  ENNHCPASSESHPKPSSPRQESTRVIQLMPSPIMHPLILNPRHSVDFKQSRLSEDGLHRE  300
TrkC             ------------------------------------------------------------

fusion     301  GKPINLSHREDLAYMNHIMVSVSPPEEHAMPIGRIAGPVAVISGEEDSASPLHHINHGIT  360
TEL        301  GKPINLSHREDLAYMNHIMVSVSPPEEHAMPIGRIA------------------------  336
TrkC       466  ----------------------------------GPVAVISGEEDSASPLHHINHGIT  489

fusion     361  TPSSLDAGPDTVVIGMTRIPVIENPQYFRQGHNCHKPDTYVQHIKRRDIVLKRELGEGAF  420
TEL             ------------------------------------------------------------
TrkC       490  TPSSLDAGPDTVVIGMTRIPVIENPQYFRQGHNCHKPDTYVQHIKRRDIVLKRELGEGAF  549

fusion     421  GKVFLAECYNLSPTKDKMLVAVKALKDPTLAARKDFQREAELLTNLQHEHIVKFYGVCGD  480
TEL             ------------------------------------------------------------
TrkC       550  GKVFLAECYNLSPTKDKMLVAVKALKDPTLAARKDFQREAELLTNLQHEHIVKFYGVCGD  609

fusion     481  GDPLIMVFEYMKHGDLNKFLRAHGPDAMILVDGQPRQAKGELGLSQMLHIASQIASGMVY  540
TEL             ------------------------------------------------------------
TrkC       610  GDPLIMVFEYMKHGDLNKFLRAHGPDAMILVDGQPRQAKGELGLSQMLHIASQIASGMVY  669

fusion     541  LASQHFVHRDLATRNCLVGANLLVKIGDFGMSRDVYSTDYYRVGGHTMLPIRWMPPESIM  600
TEL             ------------------------------------------------------------
TrkC       670  LASQHFVHRDLATRNCLVGANLLVKIGDFGMSRDVYSTDYYRVGGHTMLPIRWMPPESIM  729

fusion     601  YRKFTTESDVWSFGVILWEIFTYGKQPWFQLSNTEVIECITQGRVLERPRVCPKEVYDVM  660
TEL             ------------------------------------------------------------
TrkC       730  YRKFTTESDVWSFGVILWEIFTYGKQPWFQLSNTEVIECITQGRVLERPRVCPKEVYDVM  789

fusion     661  LGCWQREPQQRLNIKEIYKILHALGKATPIYLDILG                          696
TEL             ----------------------------------
TrkC       790  LGCWQREPQQRLNIKEIYKILHALGKATPIYLDILG                          825
```

Supplementary Fig. S8. Fusion junction sequence and predicted protein sequences of the acquired fusion in patient 784. Sanger sequencing of the junction and predicted protein sequence of the fusion ETV6-NTRK3. Highlighted conserved protein domains: turquoise: SAMpointed domain and green: protein tyrosine kinase. NCBI IDs used for the alignments: TEL: NP_001978; TrkC: NP_002521.

A

Patient 784

FLT3-ITD #1 (42 bp) 784_0

CAATTTAGGTATGAAAGCCAGCTACAGATGGTACAGGTGACCGGCTCCTCAGATAATGAGT
ACTTCTACGTTGATTTCAGAGAATATGAATATGATCTCAAATGGGAGTTTCCTGATTTCAGA
GAATATGAATATGATCTCAAATGGGAGTTTCCAAGAGAAAATTTAGAGTTTG

FLT3-ITD #2 (36 bp) 784_0

CAATTTAGGTATGAAAGCCAGCTACAGATGGTACAGGTGACCGGCTCCTCAGATAATGAGT
ACTTCTACGTTGATTTCGGCTCCTCAGATAATGAGTACTTCTACGTTGATTTCAGAGAATATG
AATATGATCTCAAATGGGAGTTTCCAAGAGAAAATTTAGAGTTTG

B

784 sample	Day	FLT3-ITD #1 (42 bp)	FLT3-ITD #2 (36 bp)
784_0	0	100.000%*	100.000%*
	88	0.800%	0.500%
	123	0.009%	0.05-0.001%
	143	0.020%	0.030%
784_1	150	NA	NA
784_2	192	NA	NA

Supplementary Fig. S9. Sequences of the FLT3-ITDs in exon 14 of patient 784. (**A**) Normal sequence of exon 14 is shown in turquoise, duplicated regions are shown in yellow, the normal instance of the duplicated sequence is underlined and the junction reads are highlighted in red. (**B**) qPCR MRD assay results for FLT3-ITD for patient 784 are depicted as the relative amount of each FLT3-ITD reported as a percentage of the amount detected in a reference sample (indicated by *). N/A indicates no sample material left for retrospective qPCR analysis.

Supplementary Table 4: Responses of DSRT guided treatment in 8 patients

Patient	DSRT-guided treatment	Treatment duration (days)	Disease state at treatment start	Treatment response	Additional information	Time to progression (weeks)	Treatment related toxicity
252	Dasatinib	59	Relapsed, resistant disease	RD	Bone marrow blasts: 65-40-75%	8	Pneumonitis (gr 2)
560	Dasatinib-temsirolimus	34	Relapsed, remission	RD	Induction w. plerixafor-MAC	4	No
560	Dasatinib-sunitinib	5	Relapsed, resistant disease	RD	Blood blasts 34-0%	N/A	Neutropenic fever, diarrhea (*Campylobacter jejuni*) (gr3)
600	Dasatinib-sunitinib-temsirolimus	44	Relapsed, resistant disease	CRi		6	Diarrhea (gr 3), perineal infection (gr 2)
718	Sorafenib-clofarabine	63	Relapsed, resistant disease	Morphologic leukemia-free state	Hypoplasia	Lost to follow-up	Bone marrow hypocellularity (gr 4)
784	Dasatinib-sunitinib-temsirolimus	13	Resistant disease	RD	Bone marrow blasts: 70-35-85%	Not evaluable	Infection (gr 2)
800	Dasatinib-clofarabine-vinblastine	6	Resistant disease	Morphologic leukemia-free state	Hypoplasia	Hypoplasia, no disease progression	Infection (gr 4), death in aplasia (gr 5)
1145	Ruxolitinib-dexamethasone	48	Relapsed, resistant disease	RD	Hematologic improvement	6	Infection (gr 2)

Definitions of response are based on the European LeukemiaNet criteria. The treatment related toxicity was rated by Common Terminology Criteria for Adverse Events (CTCAE, Version 4.02). CRi: complete remission with incomplete platelet recovery, RD: refractory disease, MAC: mitoxantrone, cytarabine, etoposide.

Supplementary Table S5: Mutation spectrum in patient 600

								Exome sequencing												Amplicon-sequencing				
Chrom	Position	Reference	Variant	Variant label	Gene_Name	Transcript	Effect	NormalRefReads	NormalVarReads	NormalVarFreq %	TumorRefReads 600_0	TumorRefReads 600_2	TumorRefReads 600_3	TumorVarReads 600_0	TumorVarReads 600_2	TumorVarReads 600_3	TumorVarFreq 600_0 %	TumorVarFreq 600_2 %	TumorVarFreq 600_3 %	Normal VarFreq %	600_1 TumorVarFreq %	600_2 TumorVarFreq %	600_3 TumorVarFreq %	Group
chr11	48367455	G	A		RP11-397M16.4.1	ENST00000415304	EXON	12	1	7.69	24	25	3	15	13	8	38.46	34.21	72.73					1
chr10	95405745	G	T		PDE6C	ENST00000371447	NON_SYNONYMOUS_CODING	233	1	0.43	182	254	132	140	196	67	43.48	43.56	33.67	1.2	45.5	44.3	40	1
chr3	75715202	G	C		FRG2C	ENST00000308062	UTR_3_PRIME	14	1	6.67	36	18	8	29	9	4	44.62	33.33	33.33					1
chr16	71956511	AATGCCC	A		IST1	ENST00000535424	CODON_DELETION	16	0	0	30	28	9	25	11	3	46.3	28	33					1
chr4	84518775	C	T		AGPAT9	ENST00000395226	INTRON	17	0	0	19	22	12	18	7	3	48.65	24.14	20					1
chr15	80430038	C	G		SNORD112	ENST00000516072	UPSTREAM	19	1	5	28	16	13	30	24	13	51.72	60	50					1
chr5	127730894	C	T		FBN2	ENST00000262464	SYNONYMOUS_CODING	9	1	10	7	7	6	15	10	2	68.18	58.82	25					1
chr4	100869677	A	C		H2AFZ	ENST00000296417	NON_SYNONYMOUS_CODING	62	1	1.59	125	82	29	2	42	21	1.57	33.87	42	0.3	35	36.6	40.7	2
chr16	82032990	C	T		SDR42E1	ENST00000328945	NON_SYNONYMOUS_CODING	26	0	0	56	34	8	1	19	10	1.75	35.85	58.82	0.8	38.1	37.9	39.4	2
chr14	31572333	G	A		HECTD1	ENST00000261312	INTRON	40	1	2.44	91	46	21	2	41	16	2.15	47.13	43.24					2
chr11	32417914	G	GC	WT1 #1	WT1	ENST00000332351	FRAME_SHIFT	34	0	0	89	33	25	3	24	16	3.2	42.11	39.02	1	40.8	39.7	37.5	2
chr11	32417911	A	AC	WT1#4	WT1	ENST00000332351	FRAME_SHIFT	33	0	0	89	64	40	0	4	0	0	5.9	0	0	8.6	8.2	0	3
chr7	23293046	G	A		GPNMB	ENST00000435486	NON_SYNONYMOUS_CODING	100	0	0	203	202	104	0	15	5	0	6.91	4.59					3
chr11	32417942	A	AAC	WT1 #3	WT1	ENST00000332351	FRAME_SHIFT	27	0	0	72	39	23	0	7	12	0	15	34.29	0.7	21.3	20.8	32.8	3
chr19	47225542	G	T		STRN4	ENST00000391910	SYNONYMOUS_CODING	29	0	0	96	51	19	0	12	5	0	19.67	23.81					3
chr11	32417924	C	CGCCCT	WT1 #2	WT1	ENST00000332351	FRAME_SHIFT	34	0	0	79	49	37	2	6	4	2.4	10.7	9.6	0	17.2	19.2	5.1	3
chr5	95072667	C	T		RHOBTB3	ENST00000379982	SYNONYMOUS_CODING	104	0	0	216	199	129	14	0	0	6	0	0					3
chr1	12855740	C	A		PRAMEF1	ENST00000332296	SYNONYMOUS_CODING	43	0	0	80	62	24	13	5	1	13.98	7.46	4					3
chr4	72620865	C	CTATTTATT		RN5S163	ENST00000410304	DOWNSTREAM	56	0	0	75	77	22	21	9	6	21.88	10.4	20.6					3
chr9	137017123	C	T		WDR5	ENST00000425041	SYNONYMOUS_CODING	25	1	3.85	40	70	25	20	0	0	33.33	0	0					4
chr1	152327667	C	T		FLG2	ENST00000388718	SYNONYMOUS_CODING	14	0	0	26	29	10	13	1	1	33.33	3.33	9.09					4
chr17	40489711	T	A		STAT3	ENST00000264657	INTRON	12	0	0	23	28	10	16	0	0	41.03	0	0					4

Supplementary Table S6: Mutation spectrum in patient 784

							Exome-sequencing												Amplicon-sequencing			
Chromosome	Position	Reference	Variant	Gene_Name	Transcript	Effect	NormalRefReads	NormalVarReads	NormalVarFreq %	TumorRefReads 784_0	TumorRefReads 784_1	TumorRefReads_2	TumorVarReads 784_0	TumorVarReads 784_1	TumorVarReads 784_2	TumorVarFreq % 784_0	TumorVarFreq % 784_1	TumorVarFreq % 784_2	NormalVarFreq %	TumorVarFreq % 784_1	TumorVarFreq % 784_2	Group
chr1	87380922	A	T	RP4-604K5.1.1	ENST00000331835	UPSTREAM	10	0	0	13	3	14	17	5	13	56.67	62.5	48.15				1
chr10	35468234	G	A	CREM	ENST00000395895	INTRON	65	0	0	89	97	97	73	40	72	45.06	29.2	42.6	1.87	37.72	48.09	1
chr12	116421392	G	A	MED13L	ENST00000281928	INTRON	24	0	0	26	29	54	18	20	31	40.91	40.82	36.47				1
chr14	106780672	T	G	IGHV4-28	ENST00000390612	EXON	17	0	0	62	23	46	28	5	11	31.11	17.86	19.3				1
chr18	52555147	A	C	RAB27B	ENST00000262094	INTRON	26	0	0	26	30	44	26	16	31	50	34.78	41.33				1
chr19	36019116	G	A	SBSN	ENST00000452271	NON_SYNONYMOUS_CODING	8	0	0	13	7	25	17	3	17	56.67	30	40.48				1
chr19	48558342	TCTCCAGAAGACCC	T	AC010458.1	ENST00000408668	UPSTREAM	12	0	0	15	8	15	10	4	6	40	33.33	28.57				1
chr20	15480579	A	G	MACROD2	ENST00000310348	INTRON	23	0	0	28	21	49	24	12	36	46.15	36.36	42.35				1
chr21	22664630	C	T	NCAM2	ENST00000400546	INTRON	44	0	0	88	62	74	68	36	84	43.59	36.73	53.16				1
chr3	49940680	C	A	MST1R	ENST00000296474	NON_SYNONYMOUS_CODING	13	0	0	11	7	22	8	7	16	42.11	50	42.11				1
chr3	167405407	C	T	PDCD10	ENST00000392750	NON_SYNONYMOUS_CODING	93	0	0	139	126	144	128	86	116	47.94	40.57	44.62	2.13	37.95	47.28	1
chr3	186522559	T	C	RP11-573D15.3.1	ENST00000434957	UPSTREAM	18	0	0	54	30	38	38	14	47	41.3	31.82	55.29				1
chr3	189590730	T	C	TP63	ENST00000264731	NON_SYNONYMOUS_CODING	27	0	0	25	47	49	38	29	52	60.32	38.16	51.49	1.93	37.45	45.78	1
chr4	38056026	CA	C	TBC1D1	ENST00000261439	INTRON	17	0	0	23	22	27	18	8	34	43.9	26.67	55.74				1
chr6	36922610	T	A	PI16	ENST00000373674	NON_SYNONYMOUS_CODING	9	0	0	26	9	18	26	7	20	50	43.75	52.63				1
chr7	2627578	CAG	C	IQCE	ENST00000402050	INTRON	12	0	0	22	8	17	21	11	14	48.84	57.89	45.16				1
chrX	79946610	C	T	BRWD3	ENST00000373275	NON_SYNONYMOUS_CODING	49	0	0	57	60	76	47	23	63	45.19	27.71	45.32	1.72	NA	46.42	1
chr16	74504052	C	CTCT	GLG1	ENST00000205061	INTRON	12	1	7.69	33	20	37	21	23	28	38.89	53.49	43.08				1
chr15	72185825	C	T	MYO9A	ENST00000424560	INTRON	23	0	0	15	12	37	7	6	44	31.82	33.33	54.32				1
chr11	32413612	T	C	WT1	ENST00000332351	SPLICE_SITE_ACCEPTOR	30	0	0	49	11	3	57	35	73	53.77	76.09	96.05	4.07	76.18	94.94	NA
chr14	80669182	C	A	DIO2	ENST00000555750	SYNONYMOUS_CODING	27	1	3.57	57	31	42	46	25	39	44.66	44.64	48.15				NA
chr18	7231736	C	T	LRRC30	ENST00000383467	SYNONYMOUS_CODING	16	0	0	36	11	19	34	2	13	48.57	15.38	40.62				NA
chr19	42083432	GAC	G	CEACAM21	ENST00000401445	INTRON	19	0	0	23	31	43	10	2	5	30.3	6.06	10.42				NA
chr2	238661932	A	T	LRRFIP1	ENST00000392000	INTRON	25	0	0	33	37	39	12	6	12	26.67	13.95	23.53				NA
chr12	11183541	T	C	TAS2R31	ENST00000390675	NON_SYNONYMOUS_CODING	68	1	1.45	187	122	208	20	20	32	9.66	14.08	13.33				NA
chr12	11214386	T	G	TAS2R46	ENST00000533467	NON_SYNONYMOUS_CODING	79	0	0	268	209	231	13	12	19	4.63	5.43	7.6				NA
chr3	75714674	G	A	RP11-413E6.7.1	ENST00000489078	UPSTREAM	34	0	0	99	47	112	13	7	27	11.61	12.96	19.42				NA

Supplementary Table S7. Primer sequences used for amplicon sequencing

Primer name	Primer sequence
PDCD10-F	5'-AATGATACGGCGACCACCGAGATCTACACTCTTTCCCTACACGACGCTCTTCCGATCTAAACAACTAGGCATAAACCAACA-3'
PDCD10-R	5'-CAAGCAGAAGACGGCATACGAGAT[AAGCTA]GTGACTGGAGTTCAGACGTGTGCTCTTCCGATCTCAACAGGGATATAGCTAGTGCAA-3'
BRWD3-F	5'-AATGATACGGCGACCACCGAGATCTACACTCTTTCCCTACACGACGCTCTTCCGATCTTTTTCAAGTCTCCGCCTGAT-3'
BRWD3-R	5'-CAAGCAGAAGACGGCATACGAGAT[TTGACT]GTGACTGGAGTTCAGACGTGTGCTCTTCCGATCTTAGATTTTGCCAGCCCTTTT-3'
CREM-F	5'-AATGATACGGCGACCACCGAGATCTACACTCTTTCCCTACACGACGCTCTTCCGATCTTGCTACCATGGCAGTACCAA-3'
CREM-R	5'-CAAGCAGAAGACGGCATACGAGAT[TACAAG]GTGACTGGAGTTCAGACGTGTGCTCTTCCGATCTGGAACAATTTAATGCCAAAACC-3'
H2AFZ-F	5'-AATGATACGGCGACCACCGAGATCTACACTCTTTCCCTACACGACGCTCTTCCGATCTGGAATCCAGGCATCCTTTAG-3'
H2AFZ-R	5'-CAAGCAGAAGACGGCATACGAGAT[TCAAGT]GTGACTGGAGTTCAGACGTGTGCTCTTCCGATCTCACTTTCTTGGTTTCAAATACTGTG-3'
PDE6C-F	5'-AATGATACGGCGACCACCGAGATCTACACTCTTTCCCTACACGACGCTCTTCCGATCTGAAAAATCCTGAATTGTATGAACC-3'
PDE6C-R	5'-CAAGCAGAAGACGGCATACGAGAT[GATCTG]GTGACTGGAGTTCAGACGTGTGCTCTTCCGATCTCGTACCTCATCCTGCAACAG-3'
SDR42E1-F	5'-AATGATACGGCGACCACCGAGATCTACACTCTTTCCCTACACGACGCTCTTCCGATCTCCTAGCTCTTTCTTGGCTTTCTC-3'
SDR42E1-R	5'-CAAGCAGAAGACGGCATACGAGAT[CTGATC]GTGACTGGAGTTCAGACGTGTGCTCTTCCGATCTGACCTTGGTCTACTGCTTTGC-3'
TP63-F	5'-AATGATACGGCGACCACCGAGATCTACACTCTTTCCCTACACGACGCTCTTCCGATCTGTGAGGGGCCGTGAGACT-3'
TP63-R	5'-CAAGCAGAAGACGGCATACGAGAT[GGAACT]GTGACTGGAGTTCAGACGTGTGCTCTTCCGATCTGCCTCCTAAAATGACACGTTG-3'
WT1_ex6-F	5'-AATGATACGGCGACCACCGAGATCTACACTCTTTCCCTACACGACGCTCTTCCGATCTCCTGGGTAAGCACACATGAA-3'
WT1_ex6-R	5'-CAAGCAGAAGACGGCATACGAGAT[ATTGGC]GTGACTGGAGTTCAGACGTGTGCTCTTCCGATCTGCTTAAAGCCTCCCTTCCTC-3'
WT1_ex8-F	5'-AATGATACGGCGACCACCGAGATCTACACTCTTTCCCTACACGACGCTCTTCCGATCTTTACCTGTATGAGTCCTGGTGTG-3'
WT1_ex8-R	5'-CAAGCAGAAGACGGCATACGAGAT[GTAGCC]GTGACTGGAGTTCAGACGTGTGCTCTTCCGATCTCCTTGTGGGCCTCACTGT-3'

Locus specific primer sequences carrying Illumina compatible adapter sequences, grafting (P5 and P7) sequence and an amplicon specific 6 bp index sequence. Locus specific primer sequences are underlined and index sequences are in brackets.

Supplementary Table S8. Primers used for fusion gene validation

Primer Name	Primer Sequence
cNUP98-NSD1-F	AGCCTTTGGGGCCCCTGGATTTA
cNUP98-NSD1-R	CCAAAAGCCACTTGCTTGGCTTCC
cMLL-ELL-F	AAGTGGCTCCCCGCCCAAGT
cMLL-ELL-R	AGGAGAACGTCCGCGCCTCT
cETV6-NTRK3-F	CTCCCCGCCTGAAGAGCACG
cETV6-NTRK3-R	GGCATCCAGTGACGAGGGCG
cSTRN-ALK-F	CGGGACAGAATTGAATCAGGGA
cSTRN-ALK-R	CGGAGCTTGCTCAGCTTGTA

Supplementary Table S9. Primers used for qPCR analysis of fusions

Primer Name	Primer Sequence
gELL-MLL-F	CAGGCAGCGCTCACTCGGAAA
gELL-MLL-R	CCTGCTTATTGACCGGAGGTGGT
gETV6-NTRK3-F	TGGTCTGGTTCACGTTTCACTG
gETV6-NTRK3-R	GTAAATCTTCTGCAAAAGGCAGCA
gSTRN-ALK-F	GCTCCTATTATCCTGTCCCTTTGA
gSTRN-ALK-R	TGGCACCATTTAGTGTCATTTAGA

Supplementary Methods

Validation of fusion genes

Fusion genes for patients 600 and 784 were confirmed by capillary sequencing of cDNA. Exon/exon fusion data from RNA sequence information, the National Center for Biotechnology Information (NCBI) nucleotide database and Primer Blast (NCI) were used to design primers for amplification across fusion junctions (Supplementary Table 8). Double-stranded cDNA was prepared using SuperScript III (Life Technologies), random hexamers and RNA extracted from patient AML samples. Fusion gene junctions were PCR amplified using the prepared cDNA, fusion gene specific primers and either Phusion or DyNazyme II DNA polymerases (Finnzymes). Following amplification, PCR products were separated on an agarose gel and the appropriate sized fragment was purified using the NucleoSpin Gel and PCR Clean-up kit (Macherey-Nagel). Purified fragments were either directly sequenced with the primers used for PCR amplification or cloned into the pCRII-TOPO vector (Life Technologies) with the resulting plasmid insert sequenced using M13 primers.

Quantitative PCR analysis of fusion genes

Genomic breakpoints of the fusion genes identified in patients 600 and 784 were identified from RNA and whole genome sequence information. Primers were designed around the breakpoint locations (Supplementary Table 9). Regions encompassing the genomic breakpoints were PCR amplified using patient DNA (600_2 and 784_2) and the PCR primers. The PCR products were separated by agarose gel electrophoresis and purified. DNA concentration was measured on the Qubit fluorometer (Life Technologies) and the molecular mass determined from the known sequence. The copy number of the fragment was calculated and serial dilutions prepared with a

background of DNA extracted from K562 cells, which did not contain the fusions of interest. Real-time PCR was performed with serial dilutions of patient DNA and iQ SYBR Green SuperMix on the CFX96 Real Time instrument (BioRad). qPCR efficiency was checked on serially diluted genomic DNA and compared to the efficiency of the standards. Genomic DNA copy number was quantified using the standard curve and expressed as copies per ng of genomic DNA

Classification of patient 600 somatic mutations

Mutations detected by exome sequencing (**Supplementary Table S5**) were classified based on the pattern of change in tumor variant frequencies during the progression of the disease (**Supplementary Fig. S5**). Group 1 consists of early somatic mutations whose frequencies remained close to 50% in all samples. Group 2 consists of relapse specific mutations that were absent or present at very low frequencies in 600_0, but have high frequencies in both relapse samples 600_2 and 600_3. Group 3 consists of mutations with less than 40% tumor variant frequency in all samples, suggesting that these are present in minor subclones. Group 4 consists of mutations specific to the major clone at diagnosis, which have high frequencies at diagnosis but are suppressed in the relapse samples.

Mutations in *WT1* exon 6

Among other mutations, exome sequencing identified 4 insertions in *WT1* exon 6 that were located within 33 bp of each other enabling phasing of the mutations. These mutations were used as subclonal markers. All of the *WT1* mutations occur in separate alleles and in total 5 *WT1* alleles were detected in the patient (wild type [wt], *WT1* #1, *WT1* #2, *WT1* #3, *WT1* #4). Exome sequence data did not show any evidence of copy number changes at the *WT1* locus. The major

clone at diagnosis was wildtype homozygous. Hence, assuming that all the subclones are diploid at the *WT1* locus, at minimum 5 separate subclones identified by the wt and mutated *WT1* alleles must be present. Tumor variant frequencies of *WT1* #1 indicate that this mutation is present in ~80% of the cells in samples 600_2 and 600_3. Since the combined allele frequencies of *WT1* #1 and *WT1* #3 exceed 50% in sample 600_3 this indicates that the *WT1* #3 mutation must be located in the second *WT1* allele in the same cells as *WT1* #1.

Inference of clonal evolution in patient 600

The pattern of clonal evolution was inferred based on integration of data from changes in tumor variant frequencies in mutations detected by exome sequencing and changes in the relative amount of *FLT3*-ITD mutations measured by qPCR. Figure 4D shows the most parsimonious model of clonal evolution supported by the mutation data.

NUP98-NSD1 fusion and group 1 mutations were present in all samples at high frequency indicating that they must have been present in the founding clone. Clone 1: The dominant clone at diagnosis evolved from the founding clone and contained mutations specific to the diagnostic sample (group 4) as well as *FLT3*-ITD #1 which was present at low frequency in subsequent relapse samples. The clone was wild type homozygous at the *WT1* locus (*wt/wt*). Clone 2 evolved from the founding clone and was characterized by acquisition of group 2, *WT1* #1 and *FLT3*-ITD #2 mutations. Clone 3 evolved from clone 2 and was characterized by acquisition of *WT1* #2 mutation. *WT1* genotype: (*WT1* #1/*WT1* #2). Clone 4 evolved from clone 2 and was characterized by acquisition of *WT1* #3 mutation. *WT1* genotype (*WT1* #1/*WT1* #3*)*. Clone 5 evolved from clone 2 by acquiring *WT1* #4 mutation. *WT1* genotype (*WT1 #1/WT1 #4)*.

Analysis of mutations in patient 784

Majority of the mutations observed in patient 784 (**Supplementary Table S6**) showed little change in mutant allele frequencies during disease progression indicating that the majority of the observed mutations were inherited from the founding clone (group 1). Relapse samples 784_1 and 784_2 showed LOH at the WT1 locus, while LOH was present at low frequency in the 784_0 sample.

Estimation of tumor content

Tumor content estimate was calculated for each sample from exome-sequencing based variant allele frequencies of mutations in group 1. Mutations occurring in regions of LOH were excluded from the calculation. Assuming that all of these mutations are heterozygous, the average frequencies of group 1 mutations in each sample were multiplied by 2 to yield the tumor content estimates below.

	600_0	600_2	600_3
Tumor content	98%	81%	76%

	784_0	784_1	784_2
Tumor content	92%	79 %	92%